

## ULTRASONIC PROPAGATION NEAR THE MAGNETIC CRITICAL POINT OF NICKEL

B. Golding and M. Barmatz

Bell Telephone Laboratories, Murray Hill, New Jersey 07974

(Received 17 June 1969)

Measurements of the attenuation and velocity of megahertz longitudinal-acoustic waves have been made near the magnetic critical point of nickel. The temperatures of the attenuation maxima and velocity minima occur below  $T_c$  and are frequency dependent. These phenomena, which have not been observed previously in a magnetic system, show striking similarities to the behavior of first sound near the  $\lambda$  point of liquid helium.

Anomalous sound propagation near magnetic critical points has been predicted theoretically and observed experimentally in many substances.<sup>1,2</sup> Previous ultrasonic investigations have associated the transition temperature with the measured attenuation maximum.<sup>3</sup> We have studied megahertz sound propagation near the critical point of nickel ( $T_c \approx 630^\circ\text{K}$ ) and have observed that the temperatures of the attenuation maxima and velocity minima occur below  $T_c$  and are frequency dependent. Although these phenomena have not been seen previously in a magnetic system, our results show striking similarities to the behavior of first sound near the  $\lambda$  point of liquid helium.<sup>4,5</sup>

In our experiments we utilized high-purity  $\langle 001 \rangle$  oriented Ni cylinders with resistivity ratios  $R_{300}/R_{4.2} \approx 1300$ . The furnace-sample-holder design allowed temperature stability of  $\pm 1$  mdeg ( $10^{-3}$  deg) for periods of several hours. Temperature was measured with a platinum resistance surface sensor in an ac bridge circuit. Changes in velocity and attenuation could be measured continuously (and simultaneously) with sensitivities  $\Delta V/V \sim 10^{-7}$  in velocity and  $\sim 5 \times 10^{-3}$  dB/cm in attenuation. Critical-point sound-attenuation measurements were made in the temperature interval  $10^{-6} < \epsilon < 3 \times 10^{-3}$ , where  $\epsilon \equiv |1 - T/T_c|$ .

The attenuation changes for  $\langle 001 \rangle$  longitudinal sound near  $T_c$  at 20 and 60 MHz are shown in Fig. 1(a). All data were taken after the establishment of equilibrium ( $\sim 0.5$  h/point). The temperature origin  $T_0$  is arbitrarily referenced to the 20-MHz attenuation peak. At these frequencies the critical attenuation is quite small and appreciable only at temperatures within a few degrees of  $T_c$ . Well below  $T_c$  we attribute the increased attenuation to arise from the presence of ferromagnetic domains. Above  $T_c$  the attenuation approached a constant background level. The corresponding velocity changes are shown in Fig. 1(b) referred to the same temperature scale as the attenuation. The temperature dependence of the sound velocity well above the transition is linear with negative

slope, but on approaching  $T_c$  the velocity undergoes a sharp decrease and passes through a minimum. The total velocity change near the transition is small,  $(\Delta V/V)_{\text{max}} \sim 3 \times 10^{-4}$ .

Close examination of the temperature region near the 20- and 60-MHz attenuation maxima and velocity minima reveals that these extrema do not occur at the same temperature. This situation is shown in Fig. 2 and may be summarized as follows: (1) The 60-MHz attenuation peak is displaced  $80 \pm 20$  mdeg below the 20-MHz peak, (2) at 20 MHz, the velocity minimum occurs  $80 \pm 15$  mdeg below the attenuation peak, and (3) the separation between 20- and 60-MHz velocity minima is  $100 \pm 20$  mdeg. These data represent the results of a number of experiments in which the velocity and attenuation were monitored continuously as the temperature was swept through the extrema at drift rates  $\sim \pm 0.5$  mdeg/min. In some instances the velocity, attenuation, and temperature were recorded simultaneously.

These phenomena have not been seen in other magnetic systems for several reasons. First, the presence of impurities tends to obscure intrinsic critical behavior near  $T_c$ .<sup>6</sup> Also, these effects, which occur very close to  $T_c$ , necessitate a higher degree of temperature resolution and stability than achieved previously. In our nickel specimens, the temperature displacement of the attenuation and velocity extrema as well as the sharpness of the 20-MHz attenuation peak indicate that impurities or imperfections do not obscure the region near  $T_c$ . In liquid helium near the  $\lambda$  point, where problems due to impurities are minimal, similar intrinsic acoustic phenomena have been observed by several investigators.<sup>4,5</sup> We suggest that the shape and amplitude of the attenuation in the region of the maximum are characteristics of the finite frequency used in the measurement, as will be discussed below in greater detail.

Our interpretation of the attenuation measurements near the peaks is based on the basic idea that, at a given frequency, the temperature of the

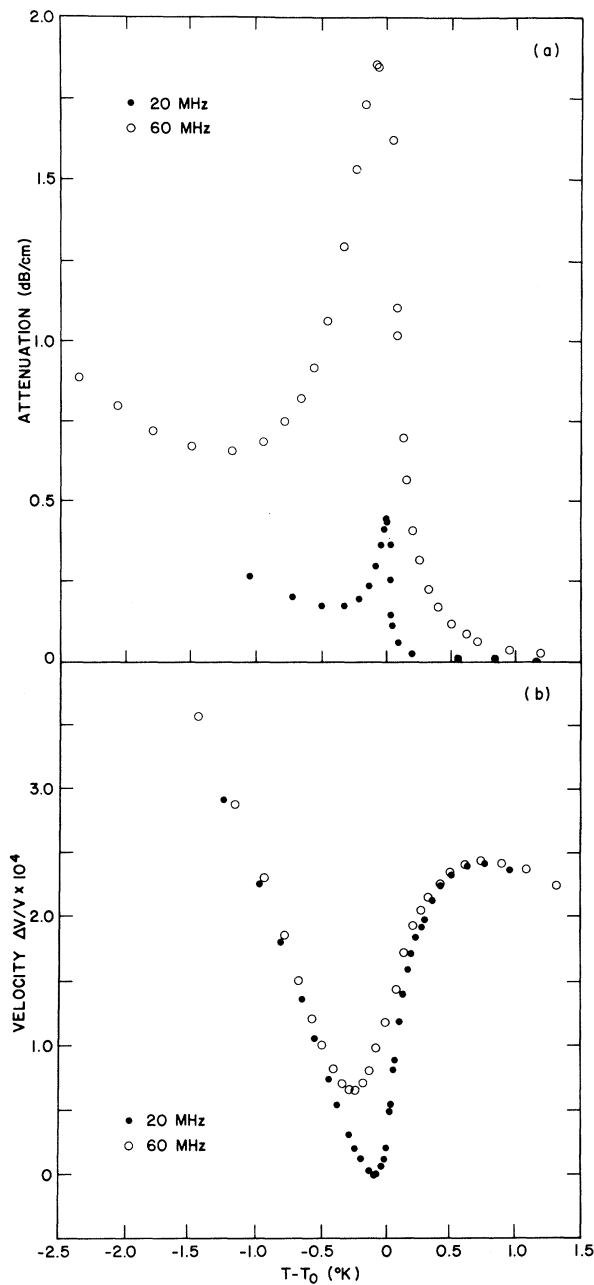


FIG. 1. Propagation of 20- and 60-MHz longitudinal sound along  $\langle 001 \rangle$  in nickel near  $T_c$ . The origin of the temperature scale  $T_0$  is arbitrarily referred to the 20-MHz attenuation peak. (a) The attenuation changes measured relative to the constant background attenuation well above  $T_c$ . (b) The dispersive effects in the velocity very near  $T_c$  can be clearly observed.

maximum attenuation divides regions of different characteristic behavior. Since the attenuation maxima shift to lower temperatures with increasing frequency, we infer that  $T_c$  lies above these extrema. In liquid helium, because of the preci-

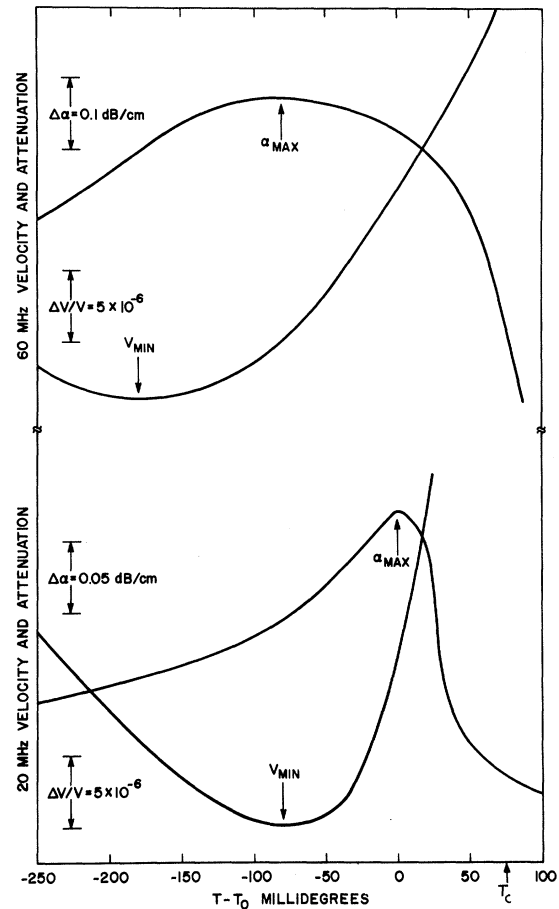


FIG. 2. Attenuation and velocity of 20- and 60-MHz sound on an expanded temperature scale near  $T_c$ . The zero of the temperature scale  $T_0$  is arbitrarily referred to the 20-MHz attenuation peak. The attenuation and velocity extrema shift to lower temperatures as the acoustic frequency increases. The arrow on the temperature axis indicates the position of  $T_c$  used in the data analysis.

sion with which  $T_\lambda$  can be measured, it is known that similar finite-frequency acoustic extrema occur below  $T_\lambda$ .

To understand our results we make use of recently proposed arguments for the application of dynamic scaling ideas to sound propagation.<sup>5,7,8</sup> We begin by recognizing the importance of the temperature-dependent critical frequency  $\omega_c$  of the critical mode,<sup>9</sup> i.e., that mode which dominates the frequency spectrum of the magnetization fluctuations at long wavelengths near the critical point. As  $T - T_c \rightarrow 0^\pm$ ,  $\omega_c^\pm \rightarrow 0$ , which implies the existence of a temperature  $T^\pm(\omega)$  at which  $\omega_c^\pm = \omega$ , where  $\omega$  is the angular sound frequency. The temperatures  $T^\pm$  divide regions with different acoustic properties.<sup>10</sup> In nickel, the

critical frequency  $\omega_c$  can be determined for  $\epsilon > 4 \times 10^{-3}$  from recent inelastic-neutron-scattering experiments.<sup>11</sup> One obtains  $\omega^+ = 1.9 \times 10^{14} \epsilon^{1.84} \text{ sec}^{-1}$  and  $\omega^- = 3.1 \times 10^{14} \epsilon^{1.72} \text{ sec}^{-1}$  which can be compared with the dynamic scaling prediction for the temperature dependence of an isotropic Heisenberg ferromagnet,  $\omega_c^{\pm} \sim \epsilon^{3\nu-\beta} \sim \epsilon^{5/3}$ , where  $\nu = \frac{2}{3}$  and  $\beta = \frac{1}{3}$ .

To indicate the validity of this interpretation we have made estimates of the attenuation-peak separation using two slightly different approaches. Using the  $\omega_c^-$  derived from the neutron-scattering measurements, we calculate the difference between  $T^-$  at 20 and 60 MHz to be 160 mdeg, a result in rather good agreement with our experimental result of  $\sim 80$  mdeg. It should be noted, however, that our measurements are confined to a region much nearer  $T_c$  than the neutron-scattering experiments. There is evidence from magnetization measurements<sup>12</sup> in Ni that the critical index  $\beta$  changes from a value near  $\frac{1}{3}$  for  $\epsilon > 5 \times 10^{-3}$  to a value near  $\frac{1}{2}$  closer to  $T_c$ . These results raise the question of the correct temperature dependence of the critical frequency for  $\epsilon < 5 \times 10^{-3}$ . We have accordingly computed the 20- and 60-MHz peak separation consistent with  $\beta = \frac{1}{2}$  and obtain a separation of  $\sim 40$  mdeg. Either calculation yields a result sufficiently consistent with experiment to give confidence in this interpretation. Using the latter temperature dependence of  $\omega_c^-$  and the experimental attenuation-peak separation, we estimate  $T_c$  to be  $\sim 75$  mdeg above the 20-MHz attenuation maximum. This choice of  $T_c$  is indicated by the arrow on the temperature axis in Fig. 2.

We assume the critical attenuation  $\alpha$  far from  $T_c$  to have the low-frequency form  $\alpha = A\omega^2\tau$ , where  $\tau$  is a relaxation time which diverges at  $T_c$  as  $\epsilon^{-\zeta}$ . A reliable measure of the temperature dependence of  $\alpha$  below  $T_c$  is complicated not only by the presence of a peak near  $T_c$  but by a non-critical attenuation probably associated with domains. For the 60-MHz measurements this non-critical contribution is approximately linear in  $T_c - T$ . An estimate of the critical exponent yields  $0 \leq \zeta < 0.2$ . Below  $T_\lambda$  in liquid helium the temperature dependence of the attenuation is the same as that of the appropriate inverse critical frequency, viz.,  $\tau = \omega_c^{-1}$ . It is clear that this relation is not valid for Ni below  $T_c$  as it predicts  $\zeta_- \approx 1.8$ . The possibility exists, therefore, that more than one relaxation time is necessary to explain the attenuation in this region.

Above  $T_c$ , we find a region in which the attenua-

tion fits a power law. In order to estimate the critical exponent  $\zeta_+$  we have analyzed the 60-MHz data in the decade  $3 \times 10^{-3} > \epsilon > 3 \times 10^{-4}$ . Using a weighted least-squares fit we obtain  $\zeta_+ = 1.4 \pm 0.1$ , where the error represents the statistical accuracy of the fit (standard error) and does not reflect the uncertainty resulting from the choice of  $T_c$ . An uncertainty of  $T_c$  of  $\pm 15$  mdeg produces a variation of  $\zeta_+$  of  $\pm 0.1$ . This measured  $\zeta$  is less than the value 1.7 obtained from the relation  $\tau = \omega_c^{-1}$ . A recent calculation of  $\zeta$  for a Heisenberg ferromagnet using the mode-mode coupling formalism<sup>13</sup> predicts  $\zeta = 5/3 - 11\alpha/6 - \frac{1}{3}\eta + \frac{1}{8}\alpha\eta \approx 1.45$ , using critical exponents appropriate for Ni. We have also made the observation that the temperature at which the 20-MHz attenuation data depart from a power law is closer to  $T_c$  than for the 60-MHz data. This result is consistent with the idea that deviations are to be anticipated when  $\omega \approx \omega_c^+$ .

The behavior of the velocity in the vicinity of  $T_c$  can be understood using an approach which has proven successful in liquid helium near the  $\lambda$  point.<sup>5</sup> The temperature dependence of the velocity near  $T_c$  arises from a thermodynamic ( $\omega = 0$ ) term and a dispersive ( $\omega \neq 0$ ) contribution. The velocity changes of the  $\langle 001 \rangle$  longitudinal mode in our experiments can be regarded, to a good approximation, as representing the changes in the adiabatic bulk modulus. It can therefore be shown that the thermodynamic velocity must (1) decrease near  $T_c$ , reflecting the increase in specific heat and (2) reach a finite minimum at  $T_c$ . For finite frequency, dispersion will increase as the transition is approached and a velocity minimum may occur at  $T \neq T_c$ , if dispersion can overcome the decrease in thermodynamic velocity. As  $\omega$  increases the minimum moves away from  $T_c$  since dispersive effects become more pronounced when  $\omega \approx \omega_c$  as can be observed in Fig. 2. A velocity minimum resulting from dispersion is not observed above  $T_c$ . This observation is due, in part, to the asymmetry in specific heat which leads to a stronger temperature dependence of the thermodynamic velocity above  $T_c$ .

In conclusion, our measurements are the first at a magnetic critical point in which intrinsic acoustic behavior very near  $T_c$  has been observed. We have shown that the critical extrema do not occur at  $T_c$  for finite frequency and that the temperatures of the attenuation maxima can be quantitatively related to the spin-wave mode. An acoustic relaxation time  $\tau$  can be related to the critical frequency  $\omega_c$  in the region well above  $T_c$ .

Below  $T_c$ , however, no similar association is possible, in contrast to the acoustic behavior of liquid helium in the region away from  $T_\lambda$ . In the near vicinity of  $T_c$  in nickel, both the attenuation and velocity of sound show features similar to those seen near  $T_\lambda$  in liquid helium.

We are indebted to P. C. Hohenberg for frequent discussions of dynamic scaling ideas. We also wish to acknowledge the experimental assistance of V. G. Chirba.

<sup>1</sup>L. P. Kadanoff, to be published.

<sup>2</sup>P. P. Craig and W. I. Goldburg [J. Appl. Phys. **40**, 964 (1969)] give an excellent review of transport properties near a magnetic transition.

<sup>3</sup>See, for example, B. Golding, Phys. Rev. Letters **20**, 5 (1968).

<sup>4</sup>C. E. Chase, Phys. Fluids **1**, 193 (1958).

<sup>5</sup>M. Barmatz and I. Rudnick, Phys. Rev. **170**, 224 (1968).

<sup>6</sup>R. J. Pollina and B. Lüthi, Phys. Rev. **177**, 841 (1969).

<sup>7</sup>B. I. Halperin and P. C. Hohenberg, Phys. Rev. **177**, 952 (1969).

<sup>8</sup>K. Kawasaki, Solid State Commun. **6**, 57 (1968), and Progr. Theoret. Phys. (Kyoto) **39**, 285 (1968).

<sup>9</sup>The critical frequency is defined as  $\omega_c = \omega_0 |k = \xi^{-1}$ , where  $\xi_0$  is the frequency of the critical mode and  $\xi$  is the correlation length. For an isotropic ferromagnet  $\omega_0$  corresponds to spin waves for  $T < T_c$  and spin diffusion for  $T > T_c$ .

<sup>10</sup>There is another dividing line defined by  $k\xi = 1$ , where  $k$  is the sound wave vector and  $\xi$  is the correlation length. For our frequency range this boundary occurs  $\sim 10^{-5}$ °K from  $T_c$  which is beyond our experimental resolution.

<sup>11</sup>M. F. Collins, V. J. Minkiewicz, R. Nathans, L. Passet and G. Shirane, Phys. Rev. **179**, 417 (1969).

<sup>12</sup>D. G. Howard, B. D. Dunlap, and J. G. Dash, Phys. Rev. Letters **15**, 628 (1965).

<sup>13</sup>G. E. Laramore, thesis, University of Illinois, 1969 (unpublished).

## PHOTOEMISSION STUDIES OF THE ELECTRONIC STRUCTURE OF EuO, EuS, EuSe, AND GdS

D. E. Eastman, F. Holtzberg, and S. Methfessel  
IBM Watson Research Center, Yorktown Heights, New York 10598  
(Received 26 June 1969)

Photoemission measurements on the magnetic semiconductors EuO, EuS, and EuSe show emission from  $4f^7$  states which lie in the gap above the top of  $\sim 2$ - to  $3$ -eV-wide valence bands. These measurements, together with optical data, indicate semiconductor energy gaps of 4.3, 3.1, and 3.1 eV for EuO, EuS, and EuSe (all  $\pm 0.4$  eV). Metallic GdS shows a narrow occupied conduction band at the Fermi level, in addition to a filled valence band and  $4f^7$  state.

The magnetic and semiconducting NaCl-type compounds EuO, EuS, EuSe, and EuTe and their solid solutions with analogous metallic compounds such as GdS are being widely investigated because of their unique magnetic, optical, and transport properties. Observed phenomena such as the Curie-temperature increase with conductivity,<sup>1</sup> giant magnetoresistance at the ferromagnetic Curie temperature,<sup>2</sup> and large absorption-edge shift with magnetic order<sup>3</sup> have been interpreted in terms of various conflicting models of the electronic structure. The position of the localized magnetic  $4f^7$  states with respect to the valence band, the width of the intrinsic semiconductor gap, and the character of the empty states at the bottom of the conduction band have been speculated about in several papers.<sup>4</sup> We have experimentally determined the occupied energy levels in EuO, EuS, and EuSe using photoemission spectroscopy, which measures absolute electron

energies with respect to the Fermi level  $E_F$ .

Photoemission energy distribution curves show narrow stationary energy states at  $\sim 3$ , 1, and 1 eV above the top of the valence bands in EuO, EuS, and EuSe, respectively, which are identified as the localized  $4f^7$  states. In metallic GdS, we have found a narrow ( $\sim 1$ -eV-wide) occupied conduction band at  $E_F$  in addition to the  $4f^7$  state and the filled valence band. This conduction band is consistent with a partially filled  $d$  band. Our measurements confirm the basic energy-band model suggested by Methfessel<sup>5</sup> for the semiconducting Eu chalcogenides, in which the  $4f^7$  state lies in the energy gap between the valence and conduction bands.

Photoemission from EuO was measured in the range  $2.5 \text{ eV} \lesssim h\nu \leq 11.6 \text{ eV}$  using a  $\langle 100 \rangle$  surface of a single crystal (with  $\sim 1$ -cm dimensions) which was prepared by cleaving in ultrahigh vacuum ( $p \lesssim 1 \times 10^{-10}$  Torr). Polycrystalline films of EuS,